

180 diffusion through amorphous SiO₂ and cristobalite

J. RodríguezViejo, F. Sibieude, M. T. ClavagueraMora, and C. Monty

Citation: *Applied Physics Letters* **63**, 1906 (1993); doi: 10.1063/1.110644

View online: <http://dx.doi.org/10.1063/1.110644>

View Table of Contents: <http://scitation.aip.org/content/aip/journal/apl/63/14?ver=pdfcov>

Published by the [AIP Publishing](#)

Instruments for advanced science

Gas Analysis



- dynamic measurement of reaction gas streams
- catalysis and thermal analysis
- molecular beam studies
- dissolved species probes
- fermentation, environmental and ecological studies

Surface Science



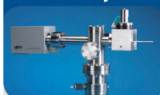
- UHV TPD
- SIMS
- end point detection in ion beam etch
- elemental imaging - surface mapping

Plasma Diagnostics



- plasma source characterization
- etch and deposition process reaction kinetic studies
- analysis of neutral and radical species

Vacuum Analysis



- partial pressure measurement and control of process gases
- reactive sputter process control
- vacuum diagnostics
- vacuum coating process monitoring

contact Hiden Analytical for further details

HIDEN
ANALYTICAL

info@hideninc.com
www.HidenAnalytical.com

CLICK to view our product catalogue 

^{18}O diffusion through amorphous SiO_2 and cristobalite

J. Rodríguez-Viejo^{a)} and F. Sibieude

Institut des Sciences et de Génie des Matériaux et Procédés, C.N.R.S. BP 5, Odeillo, 66120 Font-Romeu, France

M. T. Clavaguera-Mora

Física de Materiales, Departamento de Física, Universidad Autónoma de Barcelona, 08193 Bellaterra, Spain

C. Monty

Laboratoire de Physique des Matériaux, C.N.R.S., 1 Place Aristide Briand, Bellevue, 92195 Meudon, Cedex, France

(Received 26 January 1993; accepted for publication 6 July 1993)

Secondary ion mass spectrometry was used to profile the diffusion of oxygen in polycrystalline β -cristobalite and vitreous SiO_2 . The tracer concentration profiles of cristobalite are consistent with a model based on two mechanisms: bulk and short-circuit diffusion. The profiles of partially crystallized samples containing vitreous SiO_2 and β -cristobalite were fitted using the sum of two complementary error functions and taking account of some interstitial-network exchange. The bulk oxygen diffusivity, in the temperature range 1240–1500 °C, is about five times greater for vitreous silica than for β -cristobalite.

Vitreous silica ($\nu\text{-SiO}_2$) is an important technological material for use in dielectric thin films in integrated circuit devices and for optical elements. For this reason, numerous oxygen diffusion studies have been performed on both bulk $\nu\text{-SiO}_2$ (Refs. 1–7) and thermal oxide.^{8–17} An excellent review of oxygen mobility in silicon dioxide has been recently published by Lamkin *et al.*¹ All these studies have been made at relatively low temperatures $T < 1300$ °C, so no devitrification of the oxide occurred.

Oxygen mobility in vitreous or crystalline silica can occur, in principle, by two basic ways:¹⁵ (a) molecular oxygen permeation through the channels of open space available in these structures, or (b) oxygen self-diffusion through the network of bonded oxygens by making use of point defects. The possibility also exists that these two oxygen transport processes become interlinked by the internal exchange between the molecular oxygen interstitials and the network oxygen.

Williams² and Suco⁴ performed oxygen diffusion coefficient measurements in $\nu\text{-SiO}_2$ samples. The methods used were to follow the tracer uptake by the sample and tracer loss from the atmosphere, respectively. Although they reported similar diffusivity values at around 1000 °C, their activation energies differed greatly (1.25 and 3.09 eV), with very large differences in the preexponential factors. In the same temperature range Haul and Dumbgen,³ using the rate uptake method, found somewhat lower diffusivities with an activation energy of 2.43 eV. All these authors assumed that a single defect species was responsible for diffusion.

Cawley *et al.*¹³ and Han and Helms⁸ carried out double oxidation experiments in the range 960–1000 °C using secondary ion mass spectrometry (SIMS) to analyze tracer concentration. They found two mechanisms responsible for oxygen diffusion: interstitial molecular oxygen which exchange with the network and network oxygen diffusion.

Cawley and Boyce⁹ performed similar experiments in the range 900–1200 °C and confirmed the existence of network-interstitial exchange which is a function of temperature.

Kalen *et al.*⁵ used SIMS to profile ^{18}O tracer concentration in bulk vitreous silica and assumed two independent diffusion processes: network and interstitial. The activation energy corresponding to network oxygen diffusion was found to be 1.48 eV/atoms with a preexponential factor of $5.54 \times 10^{-11} \text{ cm}^2 \text{ s}^{-1}$.

Oxygen self-diffusion in the absence of gaseous oxygen has been measured by Mikkelsen¹⁰ using a $\text{Si}^{16}\text{O}_2\text{-Si}^{18}\text{O}_2$ thin film couple sandwich of thermal oxide. He also used SIMS to profile ^{18}O distribution. He found diffusivities several orders of magnitude below the tracer uptake data and an activation energy of 4.7 eV/atoms with a preexponential factor of $2.6 \text{ cm}^2 \text{ s}^{-1}$.

All these studies were concerned with $\nu\text{-SiO}_2$. However, to date there have not been direct measurements of oxygen diffusion in cristobalite. Nevertheless, some oxidation experiments^{16–18} have given indirect evidence about the lower diffusivity value of oxygen in cristobalite. Oxygen self-diffusion experiments in quartz^{3,19,20} and tridymite,²⁵ although the scatter in the data also show that the rates of oxygen diffusion in crystalline silicon dioxide are slower than in silica glasses.

In this study we use SIMS to profile the oxygen tracer concentration through either cristobalite or partially crystallized SiO_2 samples. The original samples used were low-water content, high-purity vitreous silica with impurities in ppm by weight: Al, 25; Li, 1; Ca, 1; Ti, 0.8; Fe, 0.5; Na, 0.5; K, 0.5; Mg, Ni, Cu, Zn < 0.1.

Since single crystals of cristobalite are unavailable only polycrystalline cristobalite was studied. It was formed by crystallization of vitreous silica.

In the diffusion experiments all starting samples ($\nu\text{-SiO}_2$ and/or polycrystalline cristobalite) were first preannealed in a high purity (< 5 ppm H_2O) oxygen-16 atmosphere during at least 15 h at the same temperature as the diffusion treatment which follow straight afterwards. The

^{a)}Permanent address: Física de Materiales, Departamento de Física, Universidad Autónoma de Barcelona, 08193 Bellaterra, Spain.

diffusion treatments were carried out by the gas-solid isotope exchange method using ^{18}O enriched gas at pressures $P=22$ and 44 kPa in the temperature range $1240\text{--}1500^\circ\text{C}$.

The preannealing time, more than 15 h at each temperature was long enough to reach thermodynamic equilibrium and to avoid any significant crystallization during the diffusion process, which lasts less than 3 h. Silica reaches a steady-state crystalline/amorphous ratio after some hours of heating depending on temperature.²⁷ This fact has been confirmed by x-ray diffraction analysis of the samples.

When the diffusion experiments were carried out at temperatures $<1400^\circ\text{C}$ two kind of samples were taken: (a) $v\text{-SiO}_2$ samples, and (b) polycrystalline cristobalite which has been produced by previous crystallization of vitreous silica at temperatures near 1500°C for 20 h. In this case, the polymorphic $\alpha=\beta$ transformation at 270°C leads to cracking of the samples when cooling down to room temperature. The average distance between cracks is $\approx 30\ \mu\text{m}$, and the grain size: $20\text{--}25\ \mu\text{m}$.

At $T > 1450^\circ\text{C}$ only initially $v\text{-SiO}_2$ samples were taken because they crystallized almost completely in cristobalite during the preannealing period.

After the experiments, samples were analyzed by x-ray diffraction, scanning electron microscopy, and SIMS. SIMS measurements were performed on a CAMECA IMS $3f$ spectrometer using a Cs^+ primary ion beam current of 200 nA or on an ATOMIKA A-DIDA 3000–30 ion microprobe using an Ar^+ primary ion beam current of 500 nA rastered over a $300\text{--}600\ \mu\text{m}^2$. All data were collected from the central 60 to $200\ \mu\text{m}^2$ region to avoid edge effects. Samples were Au coated to improve the leakage of accumulated surface charging. Moreover a focused electron gun provided charge neutralization of the sputtered surface during profiling. Three masses were simultaneously profiled: ^{16}O , ^{18}O , and $^{28,29}\text{Si}$. The SIMS crater depth was measured by means of a Talystep roughness meter.

The concentration of oxygen-18 is obtained by dividing the oxygen-18 signal by the sum of the two oxygen signals. The concentration-penetration curves corresponding to polycrystalline cristobalite samples (continuous line in Fig. 2) plotted from the SIMS profiles exhibit two different parts: A steep decrease of ^{18}O concentration for short penetrations followed by a tail. It can be deduced from these plots that two mechanisms are involved: a bulk diffusion mechanism and a short-circuit (grain boundaries or cracks) mechanism.

This kind of profile can be indeed fitted using the Whipple solution as has already been discussed by Saal *et al.*²²

$$C(y,t) = C_s \left[\operatorname{erfc} \left(\frac{\eta}{2} \right) + \frac{2\eta}{n\sqrt{\pi}} \times \int_1^\Delta \exp \left(-\frac{\eta^2}{4\sigma} \right) \left(\frac{\Delta - \sigma}{\Delta - 1} \right)^{1/2} \times \left(\frac{1}{\sqrt{\pi}} \exp(-X^2) - X \operatorname{erfc} X \right) \frac{d\sigma}{\sigma^3} \right],$$

where

$$X = \left(\frac{\Delta - 1}{\Delta - \sigma} \right)^{1/2} \frac{\sigma - 1}{2\beta}, \quad \beta = \frac{(\Delta - 1)\delta}{\sqrt{D_v t}},$$

$$\Delta = \frac{D_c}{D_v}, \quad \eta = \frac{y}{\sqrt{D_v t}}, \quad n = L(D_v t)^{1/2}.$$

The fitting parameters of this solution are D_v and D_c , the bulk and short-circuit diffusion coefficients, respectively; C_s , the constant surface concentration; δ_c , the short-circuit width and $2L$ the distance between short circuits (in noncracked polycrystals this normally corresponds to the grain size and in the cracked samples to the average distance between cracks). We also have taken into account the natural abundance of ^{18}O (0.2%).

The integral of Eq. (1) has been solved numerically using the trapezoidal rule and the Romberg interpolation method. In Fig. 1 we can see the best fitting of the experimental data using the Whipple solution. The validity of this solution has been confirmed from scanning electron microscopy measurements of the average grain size of the samples ($20\text{--}25\ \mu\text{m}$) and of the average distance between cracks ($30\ \mu\text{m}$).

The concentration-penetration curves of partially crystallized SiO_2 cannot be fitted using the Whipple solution. The presence of two phases suggests to us the sum of two complementary error functions, as previously proposed in Refs. 23, 24.

The profiles can be fitted using the solution

$$\frac{C(y,t) - C_0}{C_s - C_0} = \left\{ \left[\sum_{i=1}^2 A_i \operatorname{erfc} \left(\frac{y}{\sqrt{2D_i t}} \right) - 1 \right] \times \exp(-\gamma t) \right\} + 1, \quad (2)$$

where C_0 is the natural abundance of the tracer. The parameter A_i gives the contribution of the different diffusion coefficients to the tracer profile. The exponential term is a factor allowing for some interstitial-network exchange in the oxide ($\gamma \rightarrow$ network-interstitial coefficient), as defined by Kalen *et al.*⁵

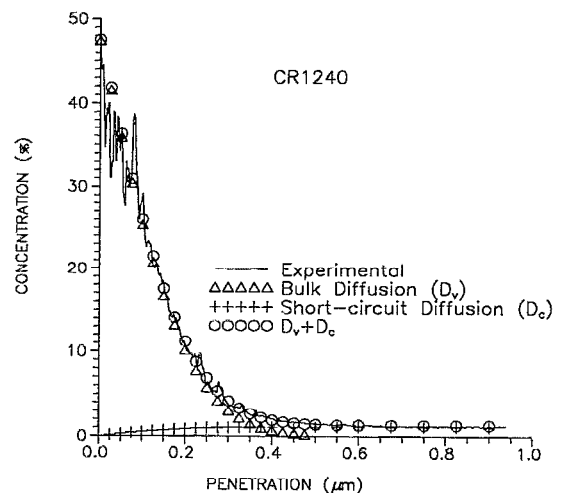


FIG. 1. Comparison between the ^{18}O experimental profile for a polycrystalline β -cristobalite sample and that calculated using the Whipple solution (Ref. CR1240).

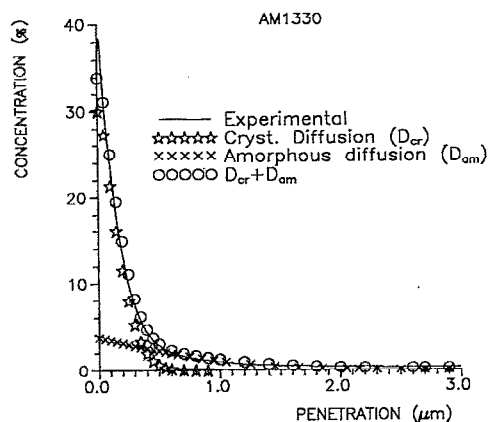


FIG. 2. Comparison between the ^{18}O experimental profile of a partially crystallized SiO_2 sample annealed in an ^{18}O enriched atmosphere at $T=1330^\circ\text{C}$ and that calculated using two complementary error functions.

A characteristic depth profile for the partially crystallized material is shown in Fig. 2. Equation (2) fits the profile very well. It is important to notice the low contribution of interstitial-network isotope exchange to the tracer profile, which can be seen from the low concentration level of the tail. In fact neglecting this phenomena would result in an overestimation of the diffusion coefficient by only a factor $\approx 2-3$.

Oxygen diffusion is slower in β -cristobalite than in vitreous silica. The bulk cristobalite data can be represented by $D_{\text{cr}} = 5.6 \text{ cm}^2 \text{ s}^{-1} \times \exp(-4.45 \text{ eV}/kT)$, whereas the amorphous by $D_{\text{am}} = 1.1 \times 10^{-2} \text{ cm}^2 \text{ s}^{-1} \times \exp(-3.4 \text{ eV}/kT)$. The activation energy for diffusion can be considered as the sum of an enthalpy of formation and an enthalpy of migration of diffusing species (interstitials, vacancies, etc.). An estimate of the enthalpy of formation of a dissociated interstitial oxygen atom and its vacancy in the SiO_2 network gives a net value of 4.4 eV.²⁵ The enthalpy of migration must only be a small part of this quantity.

A similar value for the diffusivity of ionic oxygen through oxygen vacancies in the SiO_2 network, has been proposed by Sucov,⁴ taking account of the values of Naray-Szabo.²⁶ These data agree well with the activation energy for diffusion obtained here in cristobalite.

Our diffusivity data on ν - SiO_2 is at the high side of the body of preexisting data. A direct comparison is difficult due to the large scatter in the published activation energy values. For pure network self-diffusion, Kalen *et al.* obtained an activation energy value of 1.48 eV/atoms while Mikkelsen 4.7 eV/atoms. An empirical method for comparing independently determined kinetic data is to plot the logarithm of the preexponential factor as a function of the activation energy. In such a plot our data lie between the data obtained from permeation-assisted oxygen self-diffusion in silica glass^{2-4,6} and the data for pure network self-diffusion.^{5,10} Anyway, the limited temperature range analyzed for diffusion in vitreous silica does not allow us to have much confidence in the activation energy value obtained.

With regard to the bulk oxygen diffusivity values obtained in β -cristobalite there is no self-diffusion data avail-

able. If we compare our data to those obtained from oxidation experiments,^{17,18} in a $\log D_0$ vs ΔH plot, our results agree with them.

Moreover, the diffusivity data obtained in the present work (in ν - SiO_2 and cristobalite) have been successfully used to describe the oxidation kinetics of SiC through a model which takes into account the crystallinity of the oxide layer and the existence of two diffusional paths (interstitial and network) as a function of temperature.²⁷

What is clear from this work is that network oxygen diffusion in vitreous silica is faster than in β -cristobalite. The difference of the bulk diffusivity values in β -cristobalite and ν - SiO_2 must be related to the local order of these materials. Actually, we can suppose that a small variation in the Si-O-Si angle between tetrahedra in β -cristobalite and ν - SiO_2 may induce a change either in the defect formation enthalpy or entropy. These changes could produce the difference in the diffusivity values. A better knowledge about the structure and the diffusion coefficients must be provided to clarify this problem.

The authors are very grateful to the SIMS services of the Universidad de Barcelona and the Laboratoire de Physique de Materiaux at Bellevue, for analysis of the samples. J.R. and M.T.C.-M. wish to acknowledge financial support from CICYT (Project No. MAT 92/0501).

¹F. U. Norton, *Nature* **191**, 971 (1961).

²E. L. Williams, *J. Am. Ceram. Soc.* **48**, 1903 (1965).

³R. Haul and G. Dumbgen, *Z. Elektrochem.* **66**, 636 (1962).

⁴E. Sucov, *J. Am. Ceram. Soc.* **46**, 14 (1963).

⁵J. D. Kalen, R. S. Boyce, and J. D. Cawley, *J. Am. Ceram. Soc.* **74**, 203 (1991).

⁶K. Muehlenbachs and H. A. Schaeffer, *Can. Mineral.* **15**, 179 (1977).

⁷H. A. Yinnon, Ph.D. thesis, Case Western Reserve University, OH 1979.

⁸C. J. Han and C. R. Helms, *J. Appl. Phys.* **59**, 1767 (1986).

⁹J. D. Cawley and R. S. Boyce, *Philos. Mag. A* **58**, 589 (1988).

¹⁰J. C. Mikkelsen, *Appl. Phys. Lett.* **45**, 1187 (1984).

¹¹S. S. Cristy and J. B. Condon, *J. Electrochem. Soc.* **128**, 2170 (1981).

¹²B. E. Deal and A. S. Grove, *J. Appl. Phys.* **36**, 3770 (1965).

¹³J. D. Cawley, J. W. Halloran, and A. R. Cooper, *Oxid. Metals* **28**, 1 (1987).

¹⁴A. G. Revesz and H. L. Hughes, *J. Non-Cryst. Solids* **71**, 87 (1985).

¹⁵M. A. Lamkin, F. L. Riley, and R. J. Fordham, *J. Eur. Ceram. Soc.* **10**, 347 (1992).

¹⁶J. A. Costello and R. E. Tressler, *J. Am. Ceram. Soc.* **64**, 327 (1981).

¹⁷W. Breinen, A. Naoumidis, and H. Nickel, *J. Nucl. Mater.* **71**, 56 (1977).

¹⁸T. W. Choi and H. L. Lee, *Yo Op Hoe Chi* **18**, 79 (1981).

¹⁹R. Schachtner and H. G. Sockel, in *Proceedings of the 8th International Symposium on Reactivity of Solids*, edited by J. Wood, O. Lindquist, C. Helgesson, and N. G. Vannerburg (Plenum, New York, 1977).

²⁰A. Choudhury, D. W. Palmer, G. Amsel, H. Curien, and P. Baruch, *Solid State Commun.* **3**, 119 (1965).

²¹B. E. Ramachandran, C. Bala Singh, B. C. Pai, and N. Balasubramanian, *Mater. Sci. Eng.* **67**, L5 (1984).

²²B. Saal, H. G. Sockel, and M. Heilmair, *Philos. Mag.* **61**, 801 (1990).

²³S. J. Rothman, J. L. Routbort, and J. E. Baker, *Phys. Rev. B* **40**, 8852 (1989).

²⁴J. Sabras, Ph.D. thesis, University of Paris 6, 1991.

²⁵Y. Limoge, in *Diffusion in Materials*, edited by A. L. Laskar, J. L. Bocquet, G. Brebec, and C. Monty, Aussois, France, 1990 (Kluwer Academic, Dordrecht, 1990).

²⁶I. Naray-Szabo and J. Ladik, *Nature* **188**, 226 (1960).

²⁷J. Rodriguez-Viejo, Ph.D. thesis, University of Autònoma de Barcelona, 1992.